Aswan University Journal of Science and Technology Volume 4, issue 3

Finite Element Models for Evaluating the Seismic Performance of Infilled Reinforced Concrete Frames

Amr Dahab [1], Andrew Nabeh [1], Mohamed Abdelshakour[2], Ashraf Ahmed [1], Hossameldeen Mohamed [1]
[1]Civil Engineering Department, Faculty of Engineering, Aswan University, Aswan 81542, Egypt
[2] Construction and Building Department, College of Engineering, Arab Academy for Science, Technology & Maritime Transport, Aswan , Egypt

Abstract

Masonry-infilled reinforced concrete (RC) frames are prevalent in construction due to their robust strength and durability. However, the interaction between the infill and the frame can lead to various damage patterns, complicating the assessment of their seismic performance. Both analytical and experimental studies have been carried out to examine the behavior of these structures under in-plane lateral loading. This paper proposes a simplified micro-modeling approach using the commercial software ABAQUS to simulate the behavior of infilled RC frames with local brick samples. The proposed model is validated against experimental data, showcasing its ability to predict the load-displacement response of masonry-infilled RC frame structures. This research addresses a critical aspect of construction engineering: the seismic assessment of these frames is vital for ensuring structural safety and resilience. Utilizing the Concrete Damage Plasticity (CDP) model for RC frames and the Drucker-Prager criterion for Egyptian clay bricks, the model effectively captures the complex behavior of infilled RC frames under monotonic loading. These findings enhance the understanding of the seismic behavior of these structures, offering valuable insights for better design and retrofitting strategies.

Keywords: Infill walls, RC Frame, Simplified micro-modeling, and Finite Element.

1- INTRODUCTION

Masonry, a widely used structural material, holds significant historical importance and continues to find applications in diverse construction purposes. Masonry comprises units and mortar, each possessing distinct mechanical properties. The arrangement and geometry of these constituents can vary, giving rise to various masonry configurations. Consequently, masonry is classified as a heterogeneous anisotropic material, making the analysis, understanding, and capture of its structural behavior complex. To design non-standard masonry structures or assess existing ones, numerical modeling is often necessary to comprehend the structural response under different loading conditions.

In contemporary times, numerical models provide a feasible alternative to physical experiments. Various numerical methods, such as the finite element method (FEM), discrete element method (DEM), limit analysis, and the applied element method (AEM), have been employed to conduct numerical analysis and simulate the linear and non-linear behavior of masonry. This paper focuses on the finite element method (FEM) for masonry analysis. FEM for masonry is based on two primary modeling approaches: micro-modeling and macro-modeling, with the choice dependent on the required level of accuracy and detail.

Corresponding author E-mail: amromar331@gmail.com

Received June 4, 2024, revised July 9, 2024, accepted July 14, 2024.

(ASWJST 2021/ printed ISSN: 2735-3087 and on-line ISSN: 2735-3095) https://journals.aswu.edu.eg/stjournal

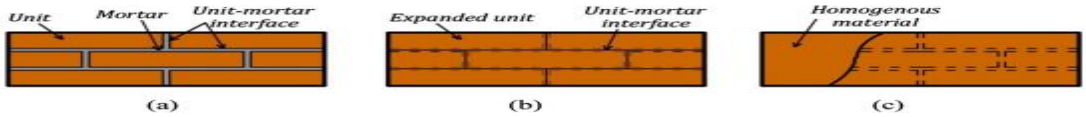

Figure 1: Finite element modeling approaches: (a) detailed Micro-model; (b) simplified Micro-model; (c) Macro-model.

In the micro-modeling approach, a detailed simulation can be conducted, where the units and mortar are modeled as continuum elements, and the interfaces between the units and mortar are modeled as discontinuum elements. The detailed micro-model, as shown in Figure 1(a), can provide accurate results but is computationally intensive and limited to simulating relatively small masonry elements. Alternatively, a simplified micro-modeling approach, as depicted in Figure 1(b), can be adopted to address the limitations of the detailed micro-model. In this simplified approach, the units are expanded by considering the mortar thickness, and the expanded units are modeled as a series of continuum elements, while the interaction between the expanded units is modeled using a series of discontinued elements.

In the macro-modeling approach, as shown in Figure 1(c), masonry is treated as a homogenous material without distinguishing between units and mortar. The material properties are derived from average properties of masonry constituents, and the masonry is modeled as a series of continuum elements. This approach is suitable for modeling relatively larger and more complex masonry structures where the global behavior is of interest, but it cannot capture detailed failure modes.

Over the past four decades, finite element techniques have continuously evolved to capture the complex structural behavior of masonry walls and associated structures. Page [1, 2] attempted to model masonry using a simplified micro-modeling approach, considering masonry units as continuum elements and mortar joints as interface elements. Shing and Cao [3] extended this approach to study the behavior of masonry assemblages by including fracture of the mortar joints into the model through interface elements. The simulation successfully captured the crack initiation and evolution of masonry mortar joints under combined normal and shear stresses in tension-shear and compression-shear regions. However, the simulation of masonry under high compression stress was unsuccessful. Lourenço and Rots [4, 5] developed a multi-surface interface model based on three yield functions: tension cut-off for tensile failure, Mohr-Coulomb failure envelope for shear failure, and a cap model for compressive failure. Additionally, potential vertical cracks were incorporated in the middle of masonry units to simulate vertical cracks under pure tension.

Shing and Cao [3] conducted finite element analysis for partially grouted masonry shear walls using a smeared crack model to simulate the fracture behavior of masonry units and plasticity-based interface elements to capture the response of mortar joints under tensile and shear stress. Although the model successfully simulated the failure modes of masonry walls, the lateral resistance of the walls was higher than the experimental results. For instance, in one of the reported models, the numerical analysis showed a 60% higher lateral resistance compared to experimental results. Sutcliffe [6] performed a lower bound limit analysis for masonry shear walls, considering both tensile and shear failure in the brick units and using a compression cap for the interface elements, but without considering material softening behavior. Citto and Kumar [7]. Developed an interface model to simulate crack initiation and propagation in masonry joints, as well as potential vertical cracks in the middle of masonry units under normal and shear stresses. The model also incorporated a compression cap to simulate the plastic response under compression. The proposed model was analyzed using ABAQUS, employing a user-defined subroutine to define the constitutive behavior. In all the aforementioned studies, simplified 2D micro-models were used to simulate only the in-plane behavior of masonry under normal and shear stresses Mohamed,H [8].

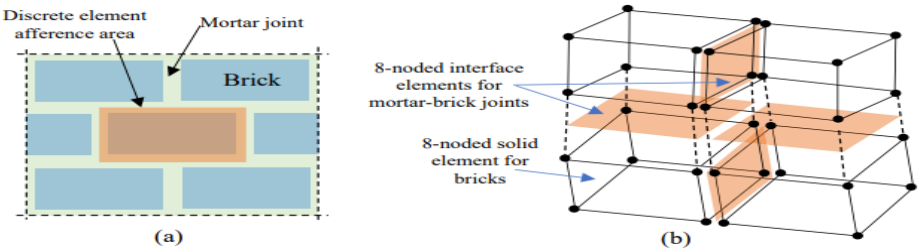

Figure 2: (a) Masonry portion describing Simplified micro scale model for masonry components (b) element model for brick units.

The studies mentioned above predominantly focused on monotonic in-plane load regimes. Oliveira and Lourenço [9] proposed a 2D model to simulate the behavior of masonry under cyclic loading using interface elements between masonry units. More recently, Miglietta [10]. Implemented a finite/discrete element model (DEM) to simulate the behavior of masonry under reversed cyclic in-plane loading. Their 2D model relied on stress-displacement relationships between adjacent masonry elements to capture the opening and sliding behavior of masonry joint elements, successfully representing the response and failure modes of masonry under reversed cyclic in-plane loading. However, the crushing of masonry under compression, which is a possible failure mode of masonry under cyclic loads, was not considered. Several studies have also been conducted to simulate the behavior of masonry under monotonic out-of-plane loads. Kuang and Yuen [11]. Performed a 3D explicit-dynamic numerical analysis using a damage-based cohesive crack model. The model, implemented in ABAQUS through a user-defined subroutine, captured the nonlinear response and failure modes of masonry-infilled reinforced concrete frames subjected to combined in-plane, out-of-plane, and dynamic loads. However, the compressive failure of masonry and cracking of masonry units were not considered. La Mendola [12]. Conducted a finite element analysis to simulate the nonlinear out-of-plane behavior of masonry. They employed interface elements with a bilinear law to simulate crack initiation and propagation in masonry joints, achieving good agreement with experimental results. However, the masonry components were modeled using an isotropic linear elastic law, neglecting possible compressive failure mechanisms. Aref and Dolatshahi [13] developed a 3D constitutive material model with an explicit-dynamic analysis procedure in ABAQUS. The model, defined through a user-defined subroutine, captured the linear and non-linear behavior of masonry under in-plane, out-of-plane, and cyclic loadings.

To summarize, most existing numerical analysis studies on masonry have focused on 2D models, limited to simulating unreinforced masonry under normal and shear stresses, and possibly out-of-plane behavior. Realistic 3D models are required to perform finite element analysis of masonry under more complex loading conditions, such as combined in-plane and out-of-plane loads experienced in service. Moreover, 3D models are essential for simulating reinforced masonry walls, as their behavior cannot be adequately captured in 2D models. Some proposed 3D models in the literature rely on user subroutines and explicit dynamic analysis procedures. Additionally, it should be noted that crack propagation within the brick units, which plays a vital role in the non-linear degradation of masonry assemblages, is either ignored or defined using interface elements, assuming potential cracks to be vertical in the middle of the units.

This paper presents a simplified 3D micro-modeling approach to simulate the behavior of masonry using the commercial finite element package ABAQUS. The proposed approach involves a combined 3D finite element model to simulate masonry walls under monotonic in-plane, out-of-plane, and cyclic in-plane loads using a quasi-static solution procedure. The model relies on surface-based cohesion with two yield criteria (tensile and shear) to simulate crack initiation and propagation in masonry joints, and a Drucker-Prager plasticity model to capture the crushing of masonry under compression. The implemented model introduces novel aspects:

1. It simulates the detailed behavior of masonry walls under in-plane and out-of-plane loads using quasi-static analyses.
2. Unlike previous approaches, it captures crack propagation within masonry units without requiring initial definition of crack locations, utilizing the extended Finite Element Method (XFEM).
3. The proposed model is simplified and user-friendly, developed by utilizing methods available in the ABAQUS Library without the need for user-defined subroutines.

2- Numerical Modeling Approach

A detailed explanation of the constitutive models used to simulate 3D masonry under a simplified modeling approach will be provided. Additionally, the failure modes associated with these models will be discussed. One of the constitutive models employed is the surface-based cohesive behavior model. This model focuses on obtaining the structural

response of masonry along bed and head joints. It captures the linear and fracture behavior of the joints by considering the traction-separation behavior between the masonry units. The surface-based cohesive model enables the simulation of failure modes in masonry joints, specifically tensile cracking and shear sliding. Tensile cracking of the joints, as shown in Fig. 3(a), is simulated by the model. When subjected to tensile loading, the model takes into account the initiation and propagation of cracks within the joints. This behavior is represented by a softening curve that describes the reduction in cohesive strength as the cracks extend. Moreover, the surface-based cohesive model also simulates shear sliding of the joints, as depicted in Fig. 3(b) and (c). When shear loading is applied to the joints, the model considers the interaction between the joint surfaces, incorporating shear tractions and separation. This allows for the representation of shear failure modes, such as sliding and separation along the joint interfaces. By including the analysis of both tensile cracking and shear sliding, the surface-based cohesive model provides a comprehensive understanding of the failure modes associated with masonry joints. Through these simulations, a more accurate depiction of the structural response of masonry can be achieved under various loading conditions.

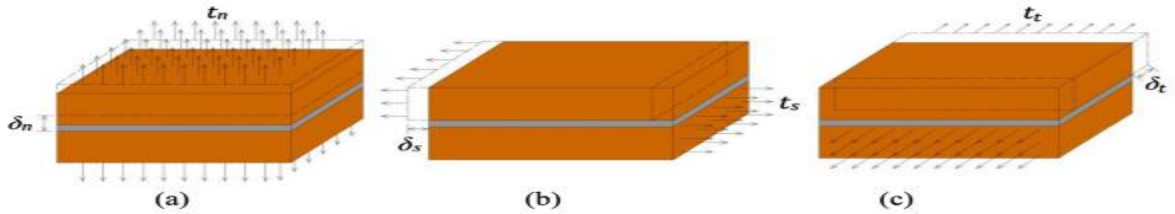

Figure 3: Failure modes of the joints: (a) tensile cracking, (b) shear sliding in x-direction, (c) Shear sliding in z-direction.

The focus is on modeling masonry units and examining five distinct failure modes that occur at the interface between bricks and mortar. These failure modes are illustrated in Figure 5 and it is crucial to accurately define and depict each mode to understand the potential mechanisms of failure. The first failure mode involves pure tensile failure, where the interface's tensile strength is surpassed. The second mode is characterized by pure sliding, where the interface slides without significant tensile failure. The third mode is a combination of cracking and shear failure along the diagonal direction. This occurs when both tensile and shear forces contribute to failure, resulting in cracks and sliding along the diagonal plane. The fourth mode entails crushing within the masonry unit itself. This happens when compressive forces exceed the brick's capacity, leading to local crushing and deformation. Lastly, the fifth mode involves cracking in the brick units, which can occur due to various factors such as material properties, structural loads, or environmental conditions. The section is divided into two subsections. The first subsection focuses on numerical modeling, particularly highlighting the modeling of mortar with cohesive properties. This entails defining the cohesive behavior and properties of the mortar interface. The subsequent subsection discusses the validation of the proposed numerical finite element (FE) model by comparing it to existing experimental studies. This validation process involves assessing the accuracy and reliability of the numerical model by comparing its predictions to experimental results obtained from tests conducted on masonry structures. By addressing the various failure modes and validating the numerical model, this section aims to provide a comprehensive understanding of masonry unit behavior and interface characteristics, enhancing the modeling approach's accuracy and reliability.

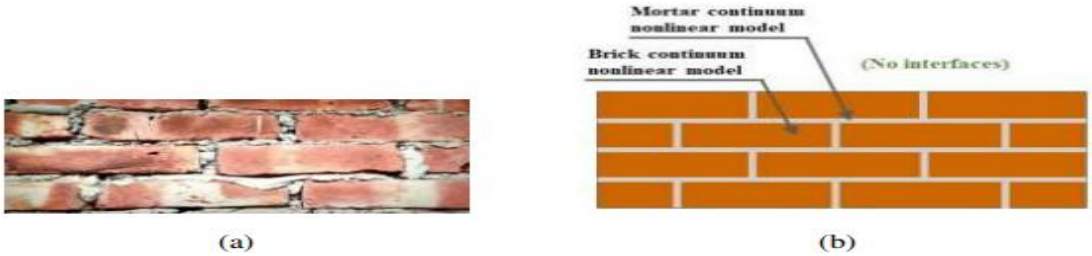

Figure 4: Modeling main strategy for brick walls a) brick wall segment, b) simplified-micro modeling.

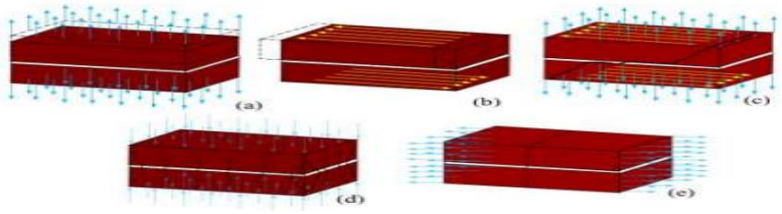

Figure 5: Crack patterns of masonry elements; a) pure tensile failure of the interface joints, b) Pure sliding shear failure at the interface, c) diagonal cracking through the assembly, d) Crushing of brick units, and e) tensile cracking failure of both brick and mortar.

The linear behavior of cohesive zone interface joints is modeled using the cohesive zone theory, which was first introduced by Dugdale [14] and further developed by Barenblatt [15]. This theory allows capturing the actual behavior of interface joints between masonry units. The cohesive element used in this study represents the interface joints and follows two basic failure modes: tensile cracking (Mode-I) and shear sliding (Mode-II/III).

To express the mechanical constitutive model of cohesive behavior, a traction-separation law is used.

$$t = k \times \delta \; where \; t = \begin{pmatrix} t_V \\ t_{HS} \\ t_{HT} \end{pmatrix}, , \mathrm{K} = \begin{bmatrix} K_V & 0 & 0 \\ 0 & K_{HS} & 0 \\ 0 & 0 & K_{HT} \end{bmatrix} \; and \; \delta = \begin{pmatrix} \delta_V \\ \delta_{HS} \\ t\delta_{HT} \end{pmatrix} \quad (1)$$

$$K_V = \frac{E_u \times E_m}{h_m \times (E_u - E_m)} \quad (2)$$

$$K_{HS} \text{ and } K_{HT} = \frac{G_u \times G_m}{h_m \times (G_u - G_m)} \quad (3)$$

The surface-based cohesive behavior can be divided into three stages: linear elastic traction-separation, damage initiation criteria, and damage evolution. The linear elastic behavior is defined by a constitutive matrix, where (*K)* represents the elastic stiffness matrix and consists of normal stiffness (K_V) and transverse stiffness's (K_{HS} and K_{HT}) of the interface elements. The nominal traction stress vector (*t*) consists of the tractions in normal and two shear directions, represented by (t_V, t_{Hs} ,and t_{HT}) respectively. The corresponding separations are denoted by (δ_V, δ_{HS}, and δ_{HT}).
The equivalent stiffness (K_V, K_{HS}, and K_{HT}) of the interface joints is defined as a function of the elasticity modulus and thickness of the brick-and-mortar elements.

$$\left(\frac{t_v}{t_v, max}\right) + \left(\frac{t_{HS}}{t_{HS}, max}\right) + \left(\frac{t_{HT}}{t_{HT}, max}\right) = 1 \quad (4)$$

The inelastic response of the masonry joints is characterized by damage initiation and propagation. Damage initiation occurs when a quadratic interaction function, based on the contact stress ratios, equals one. Tensile cracking failure is defined using the Mohr-Coulomb failure criteria, where the shear failure criteria (τ_{crit}) depends on the cohesion (*C*), friction coefficient (μ), and normal compressive stress (σ_n) Post-failure, the critical shear sliding criteria ($\tau_{sliding}$) is defined based on the law of friction, and the separation of elements leads to stiffness degradation. The damage evolution law is based on the linear softening of the fracture energy, where the damage variable (*D*) gradually increases from 0 to 1 after damage initiation. The effective separation (δ_{eff}) is defined as the combined separation in all directions. The complete failure separation (δ_{eff}, *f*) and the initial separation (δ_{eff}, 0) are used to determine the damage variable. The critical fracture energy (*GTC*) for the mixed-mode fracture law is determined by the Benzeggagh-Kenane criterion.

$$\tau_{crit} = C + \mu \times \sigma_n \quad (5)$$

$$\tau_{sliding} = \mu \times \sigma_n \quad (6)$$

$$t = (1 - D) \times [K] \times \{\delta\} \quad (7)$$

For modeling purposes, a finite element method (FEM) is proposed, where the brick elements are represented as 3D hexahedral units. Contact surfaces between masonry parts are modeled using a hard contact property, and crack propagation is simulated using the extended FEM (XFEM) method. Nonlinear geometric effects are considered, and viscosity regularization is used to mitigate numerical Instability.

$$D = \frac{\delta_{eff.f} \times (\delta_{eff.f,max} - \delta_{eff.o})}{\delta_{eff.max} \times (\delta_{eff.f} - \delta_{eff.o})} \quad (8)$$

$$\delta_{eff} = \sqrt{\delta_v{}^2 + \delta_{HS}{}^2 + \delta_{HT}{}^2} \quad (9)$$

$$\delta_{eff} = \frac{2 \times G_{TC}}{t_{eff.o}} \quad (10)$$

$$G_{TC} = G_{IC} + (G_{HC} + G_{IC}) \times \left\{\frac{G_{II}+G_{III}}{G_I+G_{II}+G_{III}}\right\}^n \quad (11)$$

$$u = \sum_{TeN} N_1(x) \times \left[u_1 + H(x) \times a_1 + \sum_{\propto=1}^{4} F_{\propto}(x) \times b_1^{\propto}\right] \quad (12)$$

2.1 Material Model for Masonry and RC Frame

Utilizing the Concrete Damage Plasticity (CDP) model for RC frames and the Drucker-Prager (D-P) criterion for Egyptian clay bricks, the model effectively captures the complex behavior of infilled RC frames under monotonic loading. The Drucker-Prager (D-P) plasticity model is employed to predict the nonlinear behavior of masonry brick units (Drucker and Prager). This model builds upon the Mohr-Coulomb criteria by analyzing the actual stresses at failure and incorporates the D-P hyperbolic function and non-associative flow rule to define the plastic flow potential (Debnath, Chen, Dhir, Ghiassi, and Paudel) [18-23]. The parameters and properties used for these models are detailed in Table 1, Table 2, and Table 3.

2.2 Meshing and Boundary Conditions

Mesh sensitivity analysis is performed to determine an appropriate number of elements. In this study, the consideration of nonlinear geometrical effects was important. To conduct numerical analysis, simplified micro-models were utilized, employing incremental displacement as a means of control. Addressing numerical instability resulting from stiffness degradation in masonry joints, the implementation of viscous regularization proved crucial. Accurate simulations required conducting mesh sensitivity analysis, ensuring the use of an appropriate number of elements to represent masonry components. A mesh size of 7 × 2 × 2 elements was determined to be practically sufficient, as further increasing mesh density had a negligible impact on the results. Abdulla [16] conducted a comprehensive examination of different viscosity parameters and mesh sizes, ultimately selecting 0.002 as the most suitable value. Consequently, this study adopted the same value for its analysis. The boundary conditions were set to reflect realistic constraints and

loading scenarios. The base of the frame was fixed to simulate a rigid foundation, and incremental horizontal displacement was applied to the top of the frame to mimic monotonic loading conditions. This setup allows for a controlled simulation of the seismic performance of the RC frames, providing valuable insights into their behavior under such loading conditions.

2.3 Interaction

The interaction between masonry units and mortar is crucial for accurate simulation. The surface-based cohesive behavior model focuses on obtaining the structural response of masonry along bed and head joints, capturing linear and fracture behavior. This includes tensile cracking and shear sliding, allowing for a comprehensive understanding of failure modes. The parameters and properties used for these models are detailed in Table 1, Table 2, and Table 3. To accurately model these interactions, the cohesive behavior model is calibrated to replicate the actual behavior observed in physical tests. This model incorporates the effects of both tensile and shears forces at the joints, which are critical in understanding how the masonry units interact under loading conditions. By capturing the linear elastic behavior and the subsequent fracture processes, the model provides a detailed depiction of how the infilled RC frames will perform under monotonic loading. This approach ensures that the simulation can predict various failure modes, such as tensile cracking and shear sliding, which are commonly observed in masonry structures. The calibration and validation of these interaction models are based on experimental data and existing literature, ensuring that the simulations are both accurate and reliable. The parameters used in these models are derived from comprehensive studies and are tailored to reflect the specific characteristics of the materials used in the construction of the frames. The detailed properties and parameters used for the interaction models are outlined in the corresponding tables, providing a clear reference for the simulation setup.

Equation (13) presents the expression for this model, where ∈ represents the coefficient denoting eccentricity, σ_{t0} signifies tensile stress, and (ψ) represents the dilation angle. Previous studies, such as Abdulla [16], have utilized this criterion to simulate masonry elements like bricks. To determine the ultimate compressive strength of the finite element (FE) models, stress-strain curves are established based on the alternating hardening and softening criteria of the (D-P) plasticity model. The eccentricity parameter (∈) is employed to define the plastic yield function and governs the rate at which the plastic flow potential approaches the asymptote. As per the Drucker-Prager theory, the plastic flow potential becomes linear when the eccentricity value approaches zero. By default, the eccentricity parameter is typically set at 0.1. In the literature, a dilatation angle of 36° is commonly assumed for unreinforced masonry structures.

$$G = \sqrt{(\in \sigma_{to} \tan\psi)^2 + q^{-2}} - \delta \tan\psi \tag{13}$$

The extended elasticity modulus ($Eadj$) is adjusted for expanded masonry units, which are larger in size compared to the actual masonry units. This adjustment is made by considering the elasticity modulus of the original masonry units and mortar, as well as the geometry of the masonry assemblage. The formula used to determine the extended elasticity modulus takes into account the even stack bond and assumes a uniform distribution of stresses in the masonry units Abdulla [16]. Equation (14) in this context incorporates the wall height (H) and the number of layers (n), while the remaining parameters are defined in the previous equations. The specific values chosen for these parameters are presented in Table 1.

$$E_{adj} = \frac{H \times E_u \times E_m}{n \times h_u \times E_m + (n-1) \times h_m \times E_u} \tag{14}$$

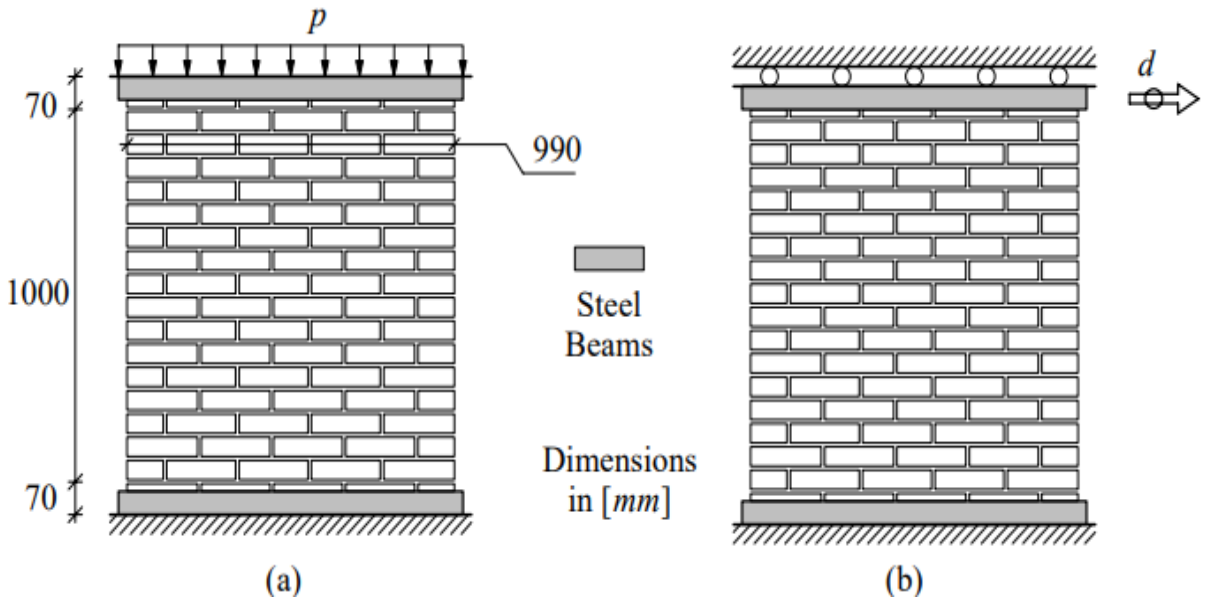

Figure 6: Loads for TU Eindhoven shear walls (a) phase vertical loading; (b) phase-Horizontal loading under displacement control.

The tests conducted on masonry shear walls as part of the CUR project in the 1990s. The tests were performed by Vermeltfoort and Raijmakers [24]. Two types of walls were investigated: those with a central opening and those without. The shear walls had a width-to-height ratio of one and dimensions of 990 × 1000 [mm²]. They were composed of 18 courses, with 16 active courses and 2 courses clamped in steel beams. The configuration of the walls is depicted in Figure 6, where the arrow with a circle represents displacement. The walls were constructed using wire-cut solid clay bricks measuring 210 × 52 × 100 [mm³], with mortar that was 10 [mm] thick. The mortar was prepared with volumetric cement: lime: sand ratio of 1:2:9.

To test the walls, different vertical recompression forces (uniformly distributed) were applied before subjecting the walls to a monotonic increase in horizontal load under top displacement control. The testing was conducted in a confined manner, meaning that the bottom and top boundaries were kept horizontal, preventing any vertical movement. This setup is also shown in Figure 6.

The material properties used in the tests were obtained from existing results of tension, compression, and shear tests, as reported of the project. Additionally, samples were collected for each specific wall to gather relevant material data.

Table 1: Elastic properties of constitutive materials and joint interfaces.

S.N.	Elastic Properties	Masonry Constitutive	Solid Walls			Remarks
			J4D and J5D	J6D	J7D	
1.	Elasticity	Brick (E_u) (MPa)	16700	16700	16700	Lourenco (1997)
		Mortar (E_m) (MPa)	780	1030	780	
		Expanded Units (MPa)	4050	4655	4655	Abdulla (2017)
2.	Poisson Ratio	Brick / Mortar	0.15	0.15	0.15	Lourenco (1997)
3.	Joint Stiffness	K_{nn} (N/mm3)	82	110	82	
		K_{ss} , K_{tt} (N/mm3)	36	50	36	

Table 2: Non-linear material properties for the joint interfaces.

Tension		Shear	
Tensile Strength (MPa)	G_f^I (N/mm)	Shear Strength (MPa)	G_f^{II} (N/mm)
2.0	0.08	2.8	0.5

Table 3: Properties for the adjusted masonry units.

S.N.	Non-linear Interface Properties		Solid Walls			Remarks
			J4D and J5D	J6D	J7D	
1.	Tension	t_{nmax} (MPa)	0.25	0.16	0.16	Lourenco (1997)
		G_f^I (N/mm)	0.018	0.018	0.018	
2.	Shear	c (MPa)	1.4 *t_{nmax}	1.4*t_{nmax}	1.4* t_{nmax}	
		μ	0.75	0.75	0.75	
		G_f^{II} (N/mm)	0.125	0.05	0.05	
3.	Compression	σ_c (MPa)	10.5	11.5	11.5	

2.4 Verification of Modeling

The proposed model is validated against experimental data, showcasing its ability to predict the load-displacement response of masonry-infilled RC frame structures. The model's accuracy and reliability are assessed by comparing its predictions to experimental results obtained from tests on masonry structures.

This validation process involves a detailed comparison of the simulation results with the empirical data. Key metrics such as peak load capacity, stiffness, and displacement at failure are evaluated. The close agreement between the numerical predictions and the experimental results demonstrates the model's capability to accurately capture the complex behavior of infilled RC frames under monotonic loading conditions.

The verification process includes:
1. **Load-Displacement Curves:** Comparing the simulated and experimental load-displacement curves to ensure the model accurately reflects the structural response.
2. **Failure Modes:** Observing the failure patterns in both the model and experiments to confirm that the model can predict realistic failure modes such as tensile cracking and shear sliding.
3. **Quantitative Analysis:** Assessing the numerical differences between the simulated results and experimental data to quantify the model's accuracy.

The validation results confirm that the proposed modeling approach, which incorporates the Concrete Damage Plasticity (CDP) model for RC frames and the Drucker-Prager criterion for masonry bricks, provides a reliable and robust simulation of the behavior of masonry-infilled RC frames. This comprehensive validation ensures that the model can be confidently used for further analysis and design of such structures.
By dividing the numerical section into these detailed subsections, each aspect of the modeling approach is thoroughly covered, providing a clear and organized presentation of the methods and results. This structured approach enhances the understanding of the simulation process and ensures that all critical components are addressed comprehensively.

3 - Numerical modeling

In order to investigate the effect of infill walls on the overall performance of RC frames, the detailed finite element modeling approach was adopted herein. ABAQUS software [25] was used to implement the modeling strategy. As such, the RC frame was modeled using 3D solid element embedded steel. Concrete Damage Plasticity (CDP) model was used for concrete and Drucker Prager (DP) for brick materials. Steel material nonlinearity was considered as bilinear model. Experimental data from the valuable research paper authored by Kakaletsis [26] were incorporated into

our analysis.

4- Results and discussion

These results were obtained under 40 mm and 20 mm monotonic loading using pushover analysis for the bare frame and masonry wall, respectively.
The results of the numerical simulation, described in Section 2, are presented graphically in Figures 7, 8, 9 and 10, depicting the horizontal top displacement versus horizontal loading for each case. It is evident from the simulation that the elastic response of the masonry wall remains consistent across all bond types. However, the non-linear behavior varies depending on the combination of aspect ratio and pre-compression load. For walls with an aspect ratio (H/L) greater than or equal to 1, ultimate failure is characterized by diagonal cracking under both pre-compression loads.

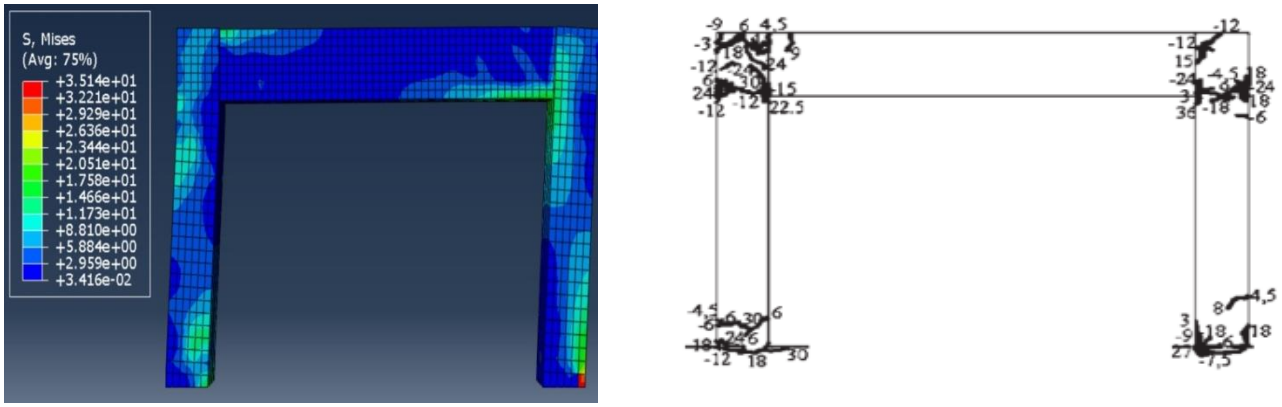

a) Numerical Model b) Experimental Data

Figure 7: the crack patterns within the selected frame. a) Numerical model, b) Experimental Data.

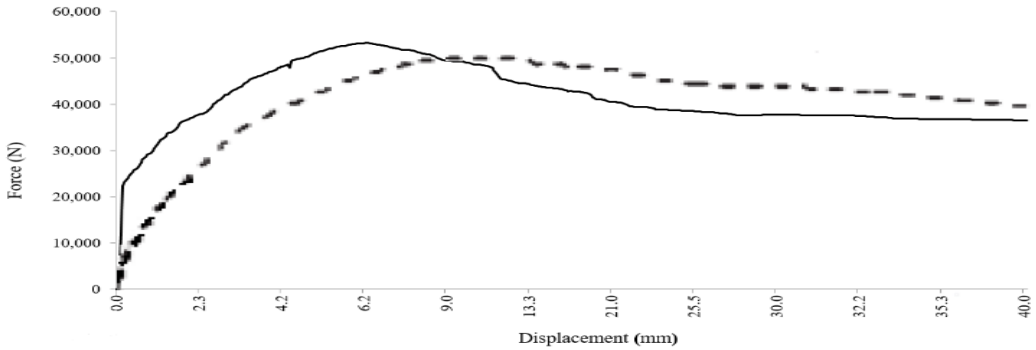

------ Experimental Model ———— Numerical Model

Figure 8: Load – Deflection Curves obtained from experimental test Kakaletsis (2008) and numerical model.

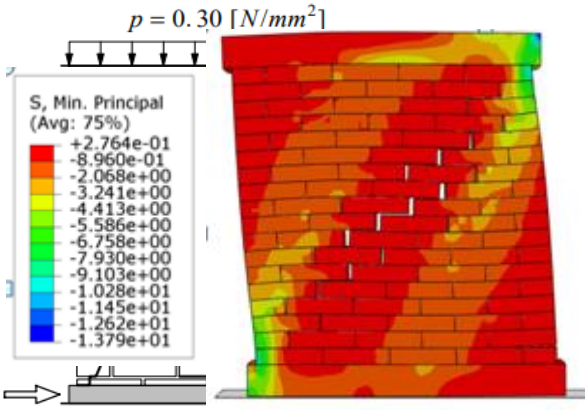

a) Experimental Data

b) Numerical Model

Figure 9: Comparison of failure modes, a) Experimental failure patterns, b) Numerical failure patterns.

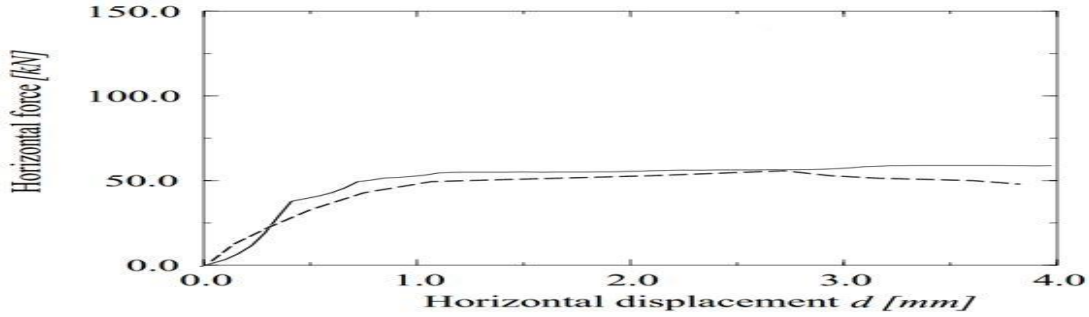

Experimental Model ——— Numerical Model

Figure 10: Load – Deflection Curves obtained from experimental test Abdulla (2017) and numerical model.

5- Conclusion

This study comprehensively explored the effects of different masonry bond types on the mechanical properties of half-brick-thick masonry walls under in-plane loading conditions. It was revealed through numerical analysis that while the elastic behavior of walls with various bond types remains consistent, significant variations are observed in their non-linear responses. The interplay between vertical and horizontal loads introduces tensile stresses that lead to distinct mechanical performances based on the bond type. It was found that walls with more head joints failed earlier than those with fewer head joints. This underscores the critical influence of bond type on the mechanical behavior and structural integrity of masonry walls.

Key Points:

1. **Consistent Elastic Behavior**: Numerical analysis showed consistent elastic behavior across various bond types.
2. **Non-Linear Response Variations**: Significant variations in non-linear responses were observed based on the bond type.
3. **Tensile Stresses and Performance**: Interplay between vertical and horizontal loads introduces tensile stresses, resulting in distinct mechanical performances.
4. **Early Failure with More Head Joints**: Walls with more head joints tend to fail earlier than those with fewer head joints, highlighting the bond type's critical influence.
5. **Design Implications**: Findings emphasize the necessity for careful consideration of bond types in the design and analysis of masonry structures to ensure resilience and reliability under load conditions.

6. **Validation and Practical Agreement**: Validation through realistic practical experiments showed good agreement with numerical modeling, enhancing confidence in the study's results.
7. **Future Research Directions**: Future research should focus on refining modeling techniques and investigating additional factors influencing masonry performance to enhance the accuracy and applicability of these findings in practical engineering scenarios.

REFERENCES

[1] A. Page, "The biaxial compressive strength of brick masonry," Proceedings of the Institution of Civil Engineers, vol. 71, no. 3, pp. 893-906, 1981.

[2] A. Page, "The strength of brick masonry under biaxial tension-compression," International Journal of Masonry Construction, vol. 3, no. 1, pp. 26-31, 1983.

[3] P. B. Shing, A. B. Mehrabi, M. Schuller, and J. L. Noland, "Experimental evaluation and finite element analysis of masonry-infilled R/C frames," in Analysis and Computation, ASCE, 1994, pp. 84-93.

[4] P. Lourenço and J. Rots, "Analysis of masonry structures with interface elements," Rep. No. 03-21-22-0 1, 1994.

[5] P. B. Lourenço and J. G. Rots, "Multisurface interface model for analysis of masonry structures," Journal of Engineering Mechanics, vol. 123, no. 7, pp. 660-668, 1997.

[6] D. J. Sutcliffe, H. S. Yu, and A. W. Page, "Lower bound limit analysis of unreinforced masonry shear walls," Computers & Structures, vol. 79, no. 14, pp. 1295-1312, 2001.

[7] C. Citto, Two-dimensional interface model applied to masonry structures, University of Colorado at Bou., 2008.

[8] H. Mohamed and X. Romão, "Assessment of the in-plane nonlinear behaviour of masonry-infilled RC frames using micro-modelling approaches," in 10º Congresso Nacional de Sismologia e Engenharia Sísmica, 2016.

[9] D. V. Oliveira and P. B. Lourenço, "Implementation and validation of a constitutive model for the cyclic behaviour of interface elements," Computers & Structures, vol. 82, no. 17-19, pp. 1451-1461, 2004.

[10] P. C. Miglietta, "Finite/discrete element modelling of reversed cyclic tests on unreinforced masonry structures," Engineering Structures, vol. 138, pp. 159-169, 2017.

[11] J. S. Kuang and Y. P. Yuen, "Simulations of masonry-infilled reinforced concrete frame failure," Proceedings of the Institution of Civil Engineers-Engineering and Computational Mechanics, vol. 166, no. 4, pp. 179-193, 2013.

[12] L. La Mendola, "Nonlinear FE analysis of out-of-plane behaviour of masonry walls with and without CFRP reinforcement," Construction and Building Materials, vol. 54, pp. 190-196, 2014.

[13] A. J. Aref and K. M. Dolatshahi, "A three-dimensional cyclic meso-scale numerical procedure for simulation of unreinforced masonry structures," *Computers & Structures, vol. 120, pp. 9-23, 2013.

[14] D. S. Dugdale, "Yielding of steel sheets containing slits," Journal of the Mechanics and Physics of Solids, vol. 8, no. 2, pp. 100-104, 1960.

[15] G. I. Barenblatt, "The mathematical theory of equilibrium cracks in brittle fracture," Advances in Applied Mechanics, vol. 7, pp. 55-129, 1962.

[16] K. F. Abdulla, "Simulating masonry wall behaviour using a simplified micro-model approach," Engineering Structures, vol. 151, pp. 349-365, 2017.

[17] D. C. Drucker and W. Prager, "Soil Mechanics and Plastic Analysis on Limit Design,"Journal of Applied Mathematics, vol. 10, pp. 157-165, 1952.

[18] P. Debnath and S. C. Dutta, "Lateral behaviour of unreinforced masonry walls with different types of opening and effect of strengthening measures: A computational approach," 2023.

[19] P. Debnath et al., "Lateral behaviour of masonry walls with different types of brick bonds, aspect ratio and strengthening measures by polypropylene bands and wire mesh," Structures, Elsevier, 2023.

[20] D. Chen et al., "Simplified micro-model for brick masonry walls under out-of-plane quasi-static and blast loadings," International Journal of Impact Engineering, vol. 174, p. 104529, 2023.

[21] P. K. Dhir et al., "Numerical modelling of reinforced concrete frames with masonry infills and rubber joints," Engineering Structures, vol. 246, p. 112833, 2021.

[22] B. Ghiassi et al., "Masonry mechanical properties," in Numerical Modeling of Masonry and Historical Structures, Elsevier, 2019, pp. 239-261.

[23] A. Paudel, G. B. Motra, and R. K. Mallik, "Technique for Non-Linear Analysis of Masonry Wall Using Discrete Crack Finite Element Method," in IOE Graduate Conference, 2020.

[24] A. T. Vermeltfoort, T. Raijmakers, and H. J. M. Janssen, "Shear tests on masonry walls," in 6th North American Masonry Conference, A. A. Hamid and H. G. Harris, Eds., Technomic Publ. Co., 1993, pp. 1183-1193.

[25] ABAQUS, ABAQUS Online Documentation, SIMULIA Inc., 2022.

[26] D. J. Kakaletsis and C. G. Karayannis, "Influence of masonry strength and openings on infilled R/C frames under cycling loading," Journal of Earthquake Engineering, vol. 12, no. 2, pp. 197-221, 2008.